Performance Evaluation of Geometric Active Contour (GAC) and Enhanced Geometric Active Contour Segmentation Model (ENGAC) for Medical Image Segmentation

Ajala Funmilola Alaba[*], Emuoyibofarhe Justice O

Department of Computer Science and Engineering, LAUTECH Ogbomoso, Oyo state, Nigeria.

*E-mail of the corresponding author: funfaith2003@yahoo.co.uk.

Abstract

Segmentation is an aspect of computer vision that deals with partitioning of an image into homogeneneous region. Medical image segmentation is an indispensable tool for medical image diagnoses. Geometric active contour (GAC) segmentation is one of the outstanding model used in machine learning community to solve the problem of medical image segmentation. However, It has problem of deviation from the true outline of the target feature and it generates spurious edge caused by noise that normally stop the evolution of the surface to be extracted.

In this paper, enhanced Geometric active contour was formulated by using Kernel Principal Component Analysis(KPCA) with the existing Geometric active contour segmentation model and performance evaluation of the formulated model was carried out.

Keyword: Geometric active contour, Segmentation, Medical image, Kernel Principal Component Analysis.

1.   Introduction

Image segmentation is an aspect of computer vision that deals with the partitioning an image into regions having homogeneous meaning. It is used to separate an object from its background and extracts meaningful objects lying in images either by dividing images into contiguous semantic regions, or by extracting one or more specific objects in images such as medical structures. However, we have different types of image segmentation methods which are not suitable for medical images since medical images are diverse, complex and vary from natural images.

Some of the methods used for medical image segmentation fall under deformable models. The use of deformable model was popularized by Kass et al. (1990), snake model was used to develop active contour model that minimizes energy functional under the influence of forces which are internal force, image force and external constraint force. Deformable models can be classified into three categories which are Free-form, Parametric and Geometric active contour model.

Geometric active contour model

This make use of level set method that represent contour or surfaces as Zero level set of a higher dimensional function usually called a level set function Chunming *et al*, (2011). Level set can handle topological changes in curve evolution which is not possible with the classical active contour model. Osher and Sethian (1998) offer a natural and numerical implementation of curve evolution equation using level set. Readers are refer to Neithammer and Tannenbum (2004) for some previous work on Geometric active contour model. Xiao *et al.,* (2003) gave the numeric scheme used for GAC model, which is describe in the following equation.

Let x= (x, y) denote a point in a curve C which is a member in image domain Ω and let the curve be represented by Lipchitz-continuous function using signed distance function. A parameterized differentiable curve C is a differential map

$$C:[a,b] \subset \Re \to \Omega = [x(p), y(p)]^T = x(p)$$

(1)

The rule that determine how each point C moves starting from initial curve C_o is

$$\frac{dC(P,t)}{dt} = v\big(C(P,t),t\big)$$ (2)

Where V = vector field that refers to as speed, Ignoring C and V in equation 2 gives

$$\frac{dC}{dt} = v$$ (3)

Equation (2) gives a partial differential equation that determines how curve C evolves and often called flow. Minimized the energy below

$$E_{image}(\phi,T) = \|H\phi - G(T)\|^2 = \int_\Omega \big(H\phi(x) - G(T,I(x))\big)^2$$ (4)

Where E_{image} is the energy that represents distance between the shape of the region defined by the interior of the curve C and the shape G extracted from the image. Effective minimization of the energy in (4) amount to realizing a trade-off between segmented object and the background.

Enhanced Geometric Active contour model

The enhanced model (ENGAC) was formulated using Kernel Principal Component Analysis (KPCA) and Geometric active contour (GAC) segmentation model. KPCA was used to get shape variability within the Geometric active contour segmentation model. The training set of MRI and CT scan of tran-axial medical images were gotten from University College Hospital, Ibadan, Oyo state. The medical images were registered using appropriate registration method to pre-process the medical images. Figure 1 gives the overview of the enhanced geometric active contour segmentation model.
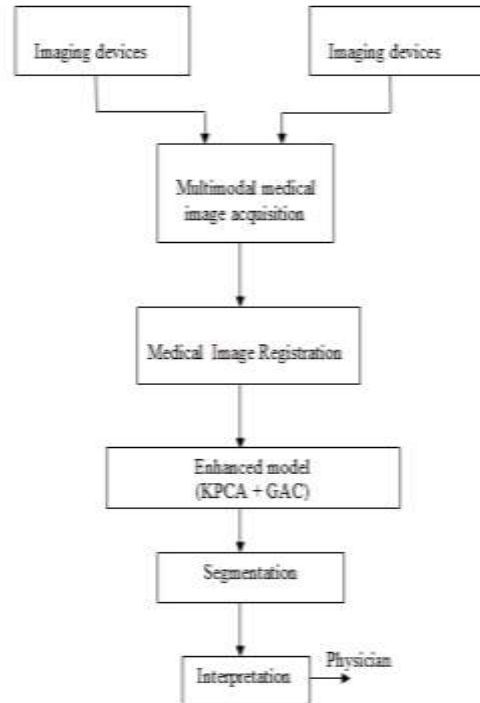

Figure 1: Overview of enhanced Geometric Active Contour model

The enhancement process started for the conventional Geometric active contour segmentation model by building Kernel Principal Component Analysis (KPCA) feature space for medical shapes to be extracted and segmented. The steps involves were;

(i)   Get a training set of registered medical images

(ii)   Represent the contour of the registered medical images with high dimensional function using signed distance function, such that a point was represented by (X_i, X_j) where $i = 1\ldots\ldots N$ and $j = 1\ldots..N$

(iii) Calculation of mean offset map represented by φ for the points using

$$\overline{\varphi} = \frac{1}{N}\sum_{i=1}^{N}\varphi\left(X_i, X_j\right)$$

(5)

(iv)   The centered kernel was formed for the points this equation

$$\overline{K}_{(i,j)} = \left(\left(\varphi(x_i)-\overline{\varphi}\right)\left(\varphi(x_j)-\overline{\varphi}\right)\right) = \left(\overline{\varphi}(x_i),\overline{\varphi}(x_j)\right) = \overline{\kappa}\left(x_i x_j\right)$$

(6)

where $\overline{\varphi}(X_i) = \varphi(X_i) - \overline{\varphi}$

(v)   The centered kernel was decomposed by getting

   (a) Diagonal matrix that represent Eigen values represented by $(\alpha_1\ldots\ldots\alpha_n)$

   (b) Orthonormal matrix that contain Eigen vectors represented by $(M_{i1}\ldots\ldots M_{iN})$

   (c) Covariance matrix calculated using $\quad C = \frac{1}{N}\sum_{i=1}^{N}\varphi\left(X_i, X_j\right)\varphi\left(X_i, X_j\right)^T$

(vi)   The Eigenvector of Covariance matrix was computed for the decomposed kernel denoted by

$$V_k = \sum_{i=1}^{N}\frac{M_{ki}}{\sqrt{\alpha_k}}\overline{\varphi}\left(X_i\right)$$

(7)

(vii) Any subsequent projection of element X of the input space I on the KPCA space was denoted by $P'\varphi(X)$ and the co-ordinate of $P'\varphi(X)$ on kth component V_k, was calculated by

$$B_k = \frac{1}{\sqrt{\gamma k}}\sum_{i=1}^{N}U_{ki}\overline{K}\left(X, X_i\right)$$

(8)

(viii) The projection of $\varphi(X)$ onto the subspace spanned by the first l eigenvectors was calculated by

$$P\varphi' = \sum_{k=1}^{l}B_k V_k + \overline{\varphi}$$

(9)

(ix)   The square distance d_F^2 between $\varphi(X)$ and its projection on the KPCA space was denoted by

$$d_F^2\left[\varphi(X), P'\varphi(X)\right] = \left\|\varphi(X) - P'\varphi(X)\right\|^2$$

(10)

To hybridize GAC and Kernel PCA, these are the steps;

(i)   Perform nonlinear PCA on the constraint SDF using Polynomial kernel function.

$$K_{\varphi_o}\left(\phi i, \phi j\right) = \left\langle\phi_i, \phi_j\right\rangle^c$$

(11)

From equation (11), when c = 2 and the square bracket is opened,

$$\left\langle\phi_i, \phi_j\right\rangle^c = \left\|\phi_i + \phi_j\right\|^2 \Rightarrow -\left\|\phi_i - \phi_j\right\|^2$$

(12)

where $\quad c =$ variance parameter.

$\left\| \phi_i - \phi_j \right\|^2$ = square distance between two SDFs Φi and Φj

φ_o = nonlinear mapping corresponding to Polynomial kernel

(2)   Minimize the energy functional equation below;

$$E^F_{energy}(x) = \left\langle \phi(x_i), Z' \varphi(x_i) \right\rangle$$

(13)

where

E^F_{energy} denotes the facts that the shape knowledge is expressed as a distance in feature space.
x = test shape represented by Signed Distance Function (SDF).
 using

$$\frac{\delta \Phi}{\delta t} = -\nabla_\Phi E^F_{energy} = -\nabla_x E^F_{energy} . \frac{dx}{d\Phi}$$

(14)

where

$$\nabla_\Phi E^F_{energy} = -\sum_{i=1}^{N} g_i (\phi) k_{\varphi o} (\phi_i, \phi_j)^c$$

2.   Methods of Performance Evaluation

The performance evaluations of the models were carried out using the following metrics by Lauren (2001). These metrics were used to evaluate the performance of enhanced Phasewire image segmentation on Livewire image segmentation.

 (a) *Segmentation/Running time*

This is the time taken to compute the segmentation including the running time of the algorithm or the time spent to perform interactive segmentation. The research was implemented on Compaq Presario CQ60 notebook PC with AMD Athlon Dual-core QL-62 2.00 GHz processor.

(b) Segmentation Accuracy

The accuracy of the segmentation algorithms is generally based on Volume measurement. This is the volume of segmented feature in the image domain. It is calculated by multiplying number of voxel by the volume of each voxel.

(c) Hausdsorff distance

This evaluating metric measures the degree of mismatch between the initial constraint and the boundary of the extracted feature. It identifies the point in one set that is the farthest from the other and outputs the distance to the nearest point in the other set. For two sets of points $A = a_1, ..., a_m$ and $B = b_1, ..., b_n$ the hausdorff distance H(A,B) is defined as;

$$H (A, B) = max(h(A, B), h(B, A))$$
Where $h(A, B) = max \ min \ || a - b ||$
            $a\varepsilon A \quad b\varepsilon B$

(d) Assessment by the Medical expert.

This is the evaluation based on Expert comment on the output of the system. The questionnaire and the system were made available for the Medical expert on the ease of usage and segmentation quality of the output

3   Discussion of Results

The training sets used for the evaluation were obtained from University College Hospital Ibadan (UCH). Trans-axial Human Brain medical images for both Computed tomography (CT) and Magnetic Resonance Imaging (MRI) were used. Figure 2(a) is a MRI scan of a human brain that serves as the test image for the registration, while Figure 2(b) is a CT scan of a human brain that was used as the refrence image for the registration. Figure 2(c) is a registered image for both CT and MRI
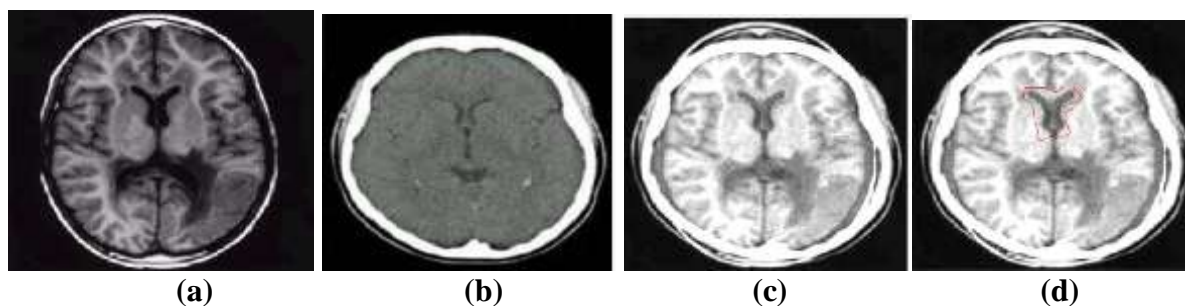

(a)   **(b)**   **(c)**   **(d)**

Figure 2: *Medical image Registration (a) MRI scan of trans-axial Human Brain (b) CT scan of trans-axial Human Brain (c) Registered image (d) Region of interest for segmentation*

(a)   (b)   (c)   (d)   (e)

(f)   (g)   (h)   (i)
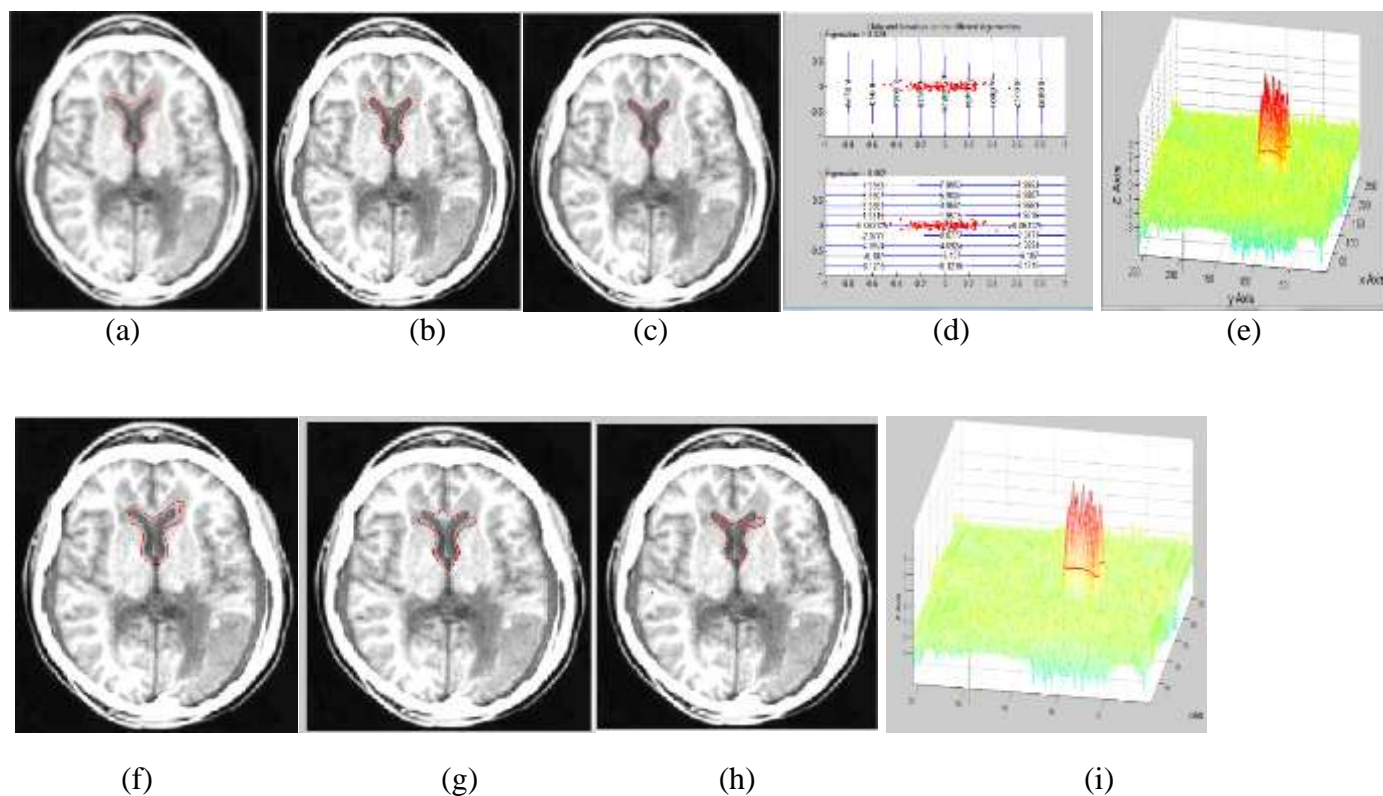
Figure 3: Segmentation Results for segmenting Caudate nucleus from trans-axial Human Brain
(GAC) *(a) contour at iteration = 100 (b) contour at iteration = 250 (c) Final segmentation contour at iteration =350 (d) magnitude of Eigenvalue (e) 3D view of segmented area.*

(ENGAC) *(f) contour at iteration = 100 (g) contour at iteration = 250 (h) Final segmentation contour   at iteration =350*
(i) 3D view of segmented area.

Figure 2(d) shows a region of interest or an initial constraint for the region to be segmented. The constraint then evolved according to specified time steps (0.005s). During the process, embedding functions continues to change the topology little by little according to the given time steps. The embedding function then reconstructed after each set of the time-steps using incremental solver in GAC. The evolving energy stops when the initial constraint minimized the energy functional to reach the shape in kernel space in ENGAC.

Figure 3(a) and (b) depict intermediate results of ENGAC Segmentation model at iteration equal 100 and 250 respectively. Figure 3(c) gives the final segmentation result at iteration equal 350. The caudate nucleus in trans-axial human brain was fully extracted using the model. Figure 3(d) gives the magnitude of Eigen value and isovalues for ENGAC image segmentation that results in a set of shape parameter vectors. From this set, the mean parameter vector and the covariance matrix as well as the Eigen vector and Eigenvalues were interpreted as mode of shape variation. At different points in the feature space on the co-ordinates x and y, x represents 0.002 and y represents 0.039. The nine (9) vectors found were represented as shown in the graph and the non-linearity of these Eigen vectors was what kernel identifies by keeping the Eigen vectors higher than tolerance of $1e^{-18}$ and by normalizing these Eigen vectors to get the exact shape. Figure 3(e) gives the 3D view of the final segmentation of the specified region of interest. This could help the physician to locate the position of caudate nucleus in the entire image domain.

Figure 3(f) and (g) depict intermediate results of GAC Segmentation model at iteration equal 100 and 250 respectively. Figure 3(h) gives the final segmentation result at iteration equal 350. The caudate nucleus in trans-axial human brain was fully extracted using the model. Figure 3(e) is the 3D view of the final segmentation of the specified region of interest

4   Performance Evaluation

The results of the performance evaluation were given below;

Segmentation time
         The segmentation time was evaluated for Geometric active contour (GAC) and enhanced Geometric active contour (ENGAC). Table 1 gives the result for the evaluation. Figure 4 shows that as the number of iteration increases the segmentation time increases for both segmentation methods but ENGAC model'segmentation time is 16.03% slower to segmentation time in Geometric Active Contour (GAC) model.

Table 1: Segmentation time for GAC model and ENGAC model for caudate nucleus segmentation in trans-axial Human Brain

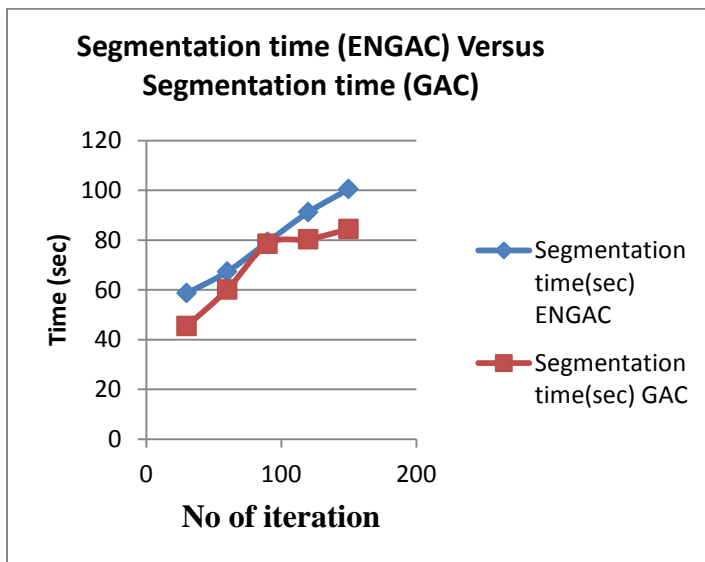| No of iteration	(ENGAC)	(GAC)
	Segmentation time(sec)	Segmentation time(sec)
30	58.65	45.42
60	67.29	60.17
90	79.31	78.49
120	91.18	80.35
150	100.49	84.38

Figure 4: Segmentation Time (ENGAC Vs GAC)

Segmentation accuracy

The segmented area volume that was used to measure the accuracy was calculated by multiplying number of voxel by the volume of each voxel. Table 2 gives the results obtained for GAC and ENGAC segmentation model. In Figure 5, as the number of iteration increases the volume area segmented decreases for both segmentation methods but ENGAC has 18.21% segmented area volume decrement compare to GAC.

Table 2: Segmented volume area for GAC model and ENGAC model for caudate nucleus segmentation in trans-axial Human Brain.

No of iteration	(ENGAC)	(GAC)
	Segmented area volume(cm^3)	Segmented area volume(cm^3)
30	5.69	5.67
60	4.55	4.71
90	4.03	4.24
120	3.12	3.85
150	3.01	3.68
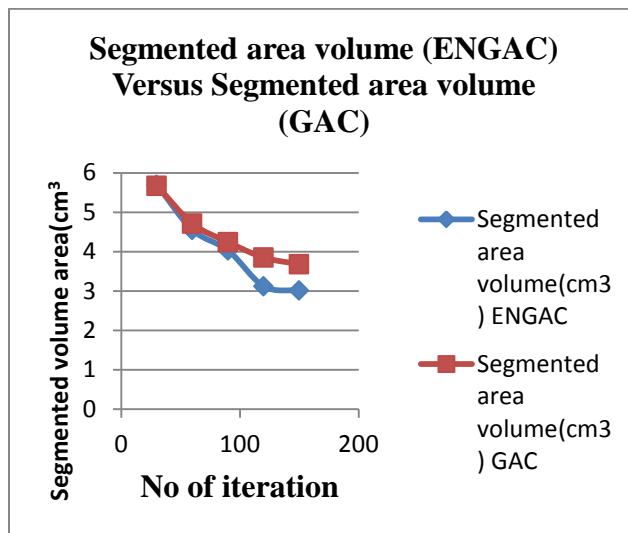
Figure 5: Segmented area volume (ENGAC Vs GAC)

Haudsorff distance

Haudsorff distance before and after segmentation was also calculated for the segmented features. Table 3(a) and (b) show the result of statistics used to quantify the nearness of the points in the initial constraint to the feature extracted. The hausdorff distance is considerably reduced in ENGAC model by 2.75mm compared to GAC model.

Table 3: Haudorff distance Before and After segmentation (a) GAC (b) ENGAC

(a)

	(GAC)	
	Before segmentation	After segmentation
Average Hausdorff distance	27.74mm	23.83mm

(b)

	(ENGAC)	
	Before segmentation	After segmentation
Average Hausdorff distance	27.81mm	21.08mm

Medical Expert's assessment

The system for ENGAC model was evaluated using likert method based on two formulated criteria which are System Ease of Use (SEU) and System Segmentation Quality (SSQ). The scale was from 1 to 5, with 5 being the highest. The response means of the methods were calculated Table 4 depicts the Medical expert's assessment for the features segmented. Segmentation quality of the ENGAC segmentation model was rated higher due to the smoothness of the contour generated at the boundary of the feature extracted follow by GAC model.

Table 4: *Medical Expert's assessment*

Study	Model	Ease of use response mean	Segmentation Quality response mean
Tran axial CT image	GAC	3.40	3.53
	ENGAC	3.42	4.25

5. Conclusion

Conclusively, GAC segmentation model is faster than ENGAC segmentation model in terms of segmentation time but ENGAC model has optimal Segmentation accuracy and quality because of its higher decrement rate in the final segmented area volume and hausdorff distance compared to Geometric active contour.

6. References

Chunming Li, Rui Huang, Zhaohua Ding, J. Chris Gatenby, Dimitris N. (2011). "A Level Set Method for Image Segmentation in the Presence of Intensity In homogeneities With Application to MRI" IEEE transactions on image processing, vol. 20, no. 7.

Chen Y, Thiruenkadam S., Tagare H., Huang F., Wilson D., and Geiser E. (2001) "On the incorporation of shape priors into geometric active contours," in *Proc. IEEE Workshop Variational and Level Set Methods*, pp. 145–152.

Wang Y. and Staib L. (1998) "Boundary finding with correspondence using statistical shape models," *IEEE Conf. Computer Vision and Pattern Recognition*, pp. 338–345.

Dambreville S., Rathi Y., and Tannenbaum A. (2008) ."A Framework for Image Segmentation Using Shape Models and Kernel Space Shape Priors," IEEE Transactions on Pattern Analysis and Machine Intelligence, 30(8):1385–99,

Charpiat G., Faugeras O., and Keriven R. (2005) "Approximations of Shape Metrics and Application to Shape Warping and Empirical Shape Statistics," Foundations of Computational Mathematics, 5(1):1–58.

Leventon M., Grimson W., and Faugeras O. (2000) "Statistical Shape Influence in Geodesic Active Contours". In Proc. IEEE CVPR.

Tsai A., Yezzi Jr A., Wells W., Tempany C., Tucker D., Fan A., Grimson W., and Willsky A. (2003) "A Shape-Based Approach to the Segmentation of Medical Imagery Using Level Sets". IEEE Trans. on Medical Imaging, 22(2):137–154.

Osher S. and Sethian J.A. (1988) "Fronts propagating with curvature dependent speed: algorithms based on Hamilton-Jacobi formulation," *Journal of Computer Physics*, vol. (79): 12-49.

Niethammer T. and Allen Tannenbaum (2004) " Dynamic Geodesic Snakes for Visual Tracking". Proceedings of the 2004 IEEE Computer Society Conference on Computer Vision and Pattern Recognition CVPR (4) : 660-667

Xiao Han, Chenyang Xu, and Jerry L. Prince, (2003) "A Topology Preserving Level Set Method for Geometric Deformable Models" IEEE Transactions on Pattern analysis and Machine intelligence, 25(6):56-70.